arXiv:hep-lat/9510047v1 26 Oct 1995

New Developments in Lattice QCD: Calculation of Flavor Singlet Nucleon Matrix Elements and Hadron Scattering Lengths

Masanori Okawa[a]

[a]National Laboratory for High Energy Physics (KEK), Tsukuba, Ibaraki 305, Japan

Recent developments in lattice QCD calculation of flavor singlet nucleon matrix elements are reviewed. Substantial sea quark contributions are found in the π-N σ term and the quark spin content of the nucleon such that the total magnitude including valence contributions is in reasonable agreement with experiments. Some problems with flavor non-singlet nucleon matrix elements are pointed out. Recent work on lattice QCD calculation of hadron scattering length is also discussed.

1. INTRODUCTION

While extensive effort has been invested for studies of the flavor non-singlet sector of strong interactions with the use of lattice QCD, attempts toward understanding the flavor singlet sector were quite limited until a few years ago [1,2]. This stemmed from the severe technical difficulty that a calculation of disconnected quark loop amplitudes, not present in the flavor non-singlet sector, requires quark propagators for a number of source points equal to the space-time lattice volume, which is prohibitively computer time consuming if it is to be carried out with the conventional method of point source.

Several methods have been developed in the last few years, however, for overcoming this problem. One of the method is a variant version of the wall source technique in which gauge configurations are not fixed to any gauge [3], as was employed in the early studies of extended sources [4]. Another is an improvement of the method of noisy source [5] with the use of a random Z_2 noise [6].

The first method has been successfully applied to estimate the flavor singlet η' meson mass in quenched QCD [7]. The method also allows a calculation of full hadron four-point functions, for which a similar computational problem is present, and hence an evaluation of hadron scattering lengths [3,8,9]. These results were available at the time of the Dallas Conference [10].

In this article we review new developments in this field since then. We devote the major part of the review to discuss recent calculations of flavor singlet nucleon matrix elements [11–18,**?**], specifically the π-N σ term and the axial vector matrix elements (quark content of proton spin). We also point out some problems with flavor non-singlet nucleon matrix elements [11] which were not apparent in the pioneering studies [20,21]. In the rest of the article we turn to some recent work on hadron scattering lengths [22,9].

Most of calculations discussed in this review are carried out in quenched QCD with the Wilson quark action. This should be understood unless stated otherwise.

2. CALCULATIONAL TECHNIQUES

A standard method for extracting the nucleon matrix element of an operator O is to employ the formula for the ratio of three- to two-point function of the nucleon and the operator given by [20]

$$\begin{aligned} R(t) \quad &= \quad \frac{\langle N(t)\sum_n O(n)\bar{N}(0)\rangle}{\langle N(t)\bar{N}(0)\rangle} \\ &\xrightarrow{t\gg 1} \quad \text{const} \ + \ Z_O^{-1}\langle N|O|N\rangle\, t, \end{aligned} \qquad (1)$$

where $N(t)$ is the nucleon operator projected to zero momentum and Z_O is the lattice renormalization factor for the operator O. For a flavor singlet quark bilinear operator $O = \overline{q}\Gamma q$, there are two types of diagrams contributing to the three-point function shown in Fig. 1. The connected amplitude can be calculated by the well known source technique [23]. To handle the dis-

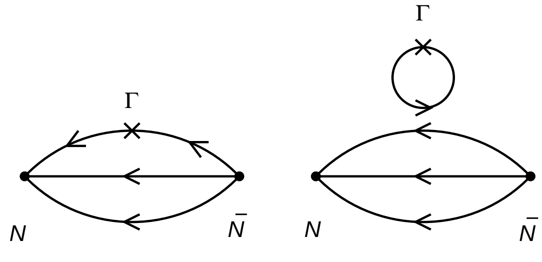

(a) connected (b) disconnected

Figure 1. (a) Connected and (b) disconnected contribution to the three-point function of nucleon and flavor singlet operator $\bar{q}\Gamma q$.

connected piece, for which the source point of the disconnected quark loop has to be summed over all space-time sites, two methods have been developed.

2.1. Wall source method without gauge fixing

In this method one calculates quark propagators with unit source at every space-time site without gauge fixing [3,11]. The result $\hat{G}(n)$ is a sum of point-to-point propagators of form

$$\hat{G}(n) \;=\; \sum_{n'} G(n;n'). \tag{2}$$

The product of the nucleon propagator and $\sum_n \mathrm{Tr}[\hat{G}(n)\Gamma]$ equals the disconnected amplitude up to gauge-variant nonlocal terms, which, however, cancel in the average over gauge configurations. Generalizing the well-known argument [24], it is possible to show that the magnitude of gauge-variant noise terms is smaller than the signal by a factor $1/\sqrt{VN}$ for a sufficiently large volume V and a number of configurations N. In practice $O(100-200)$ configurations are employed to obtain reliable signals on a lattice such as $16^3 \times 20$ at $\beta = 5.7$ [12,13].

This method requires only two quark matrix inversions for each gauge configuration, one for calculating the nucleon propagator and the other for the disconnected quark loop. Repeating the latter n times, applying random gauge transformations to a given gauge field, does not yield much gain since errors are reduced only by a factor $1/\sqrt{n}$ while the computer time grows proportional to n.

2.2. Z_2 source method

In this method [6] L quark propagators G_n^ℓ are calculated for an L set of random Z_2 source η_n^ℓ placed at every space-time site for each gauge configuration, *i.e.,*

$$G_n^\ell \;=\; \sum_{n'} G(n;n')\eta_{n'}^\ell, \quad 1 \le \ell \le L. \tag{3}$$

The product of the nucleon propagator and $\frac{1}{L}\sum_{\ell\, n} \mathrm{Tr}[G_n^\ell \eta_n^\ell \Gamma]$ equals the disconnected amplitude since $\lim_{L\to\infty} \frac{1}{L}\sum_{\ell=1}^{L} \eta_n^\ell \eta_{n'}^\ell = \delta_{nn'}$.

Employing a random source for evaluating disconnected amplitudes was previously tried for the π-N σ term for the Kogut-Susskind quark action without much success [16]. The improvement with the Z_2 noise is that the variance of the result for a finite L is smallest compared to other types of noise including the Gaussian noise.

The Z_2 source method allows a calculation of disconnected amplitudes for each configuration. However, concrete applications of the method [14,15] show that the number of quark propagators L has to be large, generally exceeding 100. Thus the method becomes harder to use for lighter quarks for which a substantial computer time is necessary to obtain even a single quark propagator.

2.3. Other methods

Some flavor singlet nucleon matrix elements can be estimated indirectly employing their relation with other quantities: (i) the scalar density matrix element can be related to the nucleon mass via Hellmann-Feynman theorem,

$$\langle N|\bar{q}q|N\rangle \;=\; \frac{dm_N}{dm_q}, \tag{4}$$

(ii) for the axial vector matrix element the $U(1)$ anomaly equation yields

$$\begin{aligned} &\langle \vec{p}, s|\bar{q}\gamma_\mu\gamma_5 q|\vec{p}, s\rangle s_\mu \\ \propto\; &\lim_{\vec{q}\to 0} \frac{1}{\vec{q}\cdot\vec{s}} \langle \vec{p}+\vec{q}, s|\mathrm{Tr}F_{\mu\nu}\tilde{F}_{\mu\nu}|\vec{p}, s\rangle. \end{aligned} \tag{5}$$

Application of these relations require full QCD simulations if disconnected contributions are to be included. In particular the anomaly relation (5) fails in quenched QCD due to the double pole

Table 1
Recent runs for nucleon matrix elements. W and KS refer to Wilson and Kogut-Susskind quarks.

	β	m_π/m_ρ	size	# conf.
singlet matrix elements				
Kyoto-Tsukuba [11–13]	5.7 (quenched W)	0.6 - 0.86	$16^3 \times 20$	260
Kentucky [14,15]	6.0 (quenched W)	0.8 - 0.95	$16^3 \times 24$	50
Altmeyer et al. [17]	5.35 ($N_f = 4$ KS)	0.46	$16^3 \times 24$	85
Gupta et al. full [18]	5.4-5.6 ($N_f = 2$ W)	0.7 - 0.85	$16^3 \times (16 \times 2)$	15 - 45
non-singlet matrix elements				
Gupta et al. [18]	6.0 (quenched W)	0.72 - 0.79	$16^3 \times 40$	35
Liu et al. [30]	6.0 (quenched W)	0.8 - 0.95	$16^3 \times 24$	24
Göckeler et al. [31]	6.0 (quenched W)	0.7 - 0.89	$16^3 \times 32$	400-1000

in the η' meson propagator connecting the disconnected quark loop and the nucleon [19]. For these reasons, only a few attempts have been made with these methods in the past [18,17].

3. NUCLEON SCALAR MATRIX ELEMENTS

3.1. π-N σ term – phenomenology

The π-N σ term is defined as the product of the nucleon matrix element of the scalar density and the average quark mass $\hat{m} = (m_u + m_d)/2$

$$\sigma(t) \;=\; \hat{m}\langle N(p')|\bar{u}u + \bar{d}d|N(p)\rangle \tag{6}$$

evaluated at $t = (p'-p)^2 = 0$, *i.e.*, $\sigma \equiv \sigma(0)$. Current algebra and PCAC relate $\sigma(t)$ to the crossing even π-N scattering amplitude at the unphysical Cheng-Dashen point $t = 2m_\pi^2$ and a dispersion analysis of π-N scattering leads to the value $\sigma(2m_\pi^2) = 64(8)$MeV [25,26].

On the other hand one can write

$$\sigma(0) \;=\; \frac{\sigma_0}{1-y}, \quad \sigma_0 = \hat{m}\langle N|\overline{u}u + \overline{d}d - 2\overline{s}s|N\rangle \tag{7}$$

with

$$y = \frac{2\langle N|\bar{s}s|N\rangle}{\langle N|\bar{u}u + \bar{d}d|N\rangle}. \tag{8}$$

Treating flavor $SU(3)$ breaking to first order, one can estimate [27]

$$\sigma_0 \approx \frac{\hat{m}}{m_s - \hat{m}}\left(M_\Xi + M_\Sigma - 2M_N\right) \approx 25\text{MeV}, \tag{9}$$

where m_s is the strange quark mass. If one assumes that the variation $\Delta_\sigma = \sigma(2m_\pi^2) - \sigma(0)$ is small, the above two estimations lead to a large strangeness content for the nucleon $y \approx 0.6$.

It has been argued, however, that the variation is substantial, $\Delta_\sigma \approx 15$ MeV [26], in which case the value of the σ term is reduced to $\sigma \approx 45$ MeV. Combined with the suggestion [28] that one-loop chiral perturbative corrections raise the value of σ_0 to $\sigma_0 \approx 35$MeV, this implies a more reasonable value $y \approx 0.2$ for the nucleon strangeness content.

Let us comment that the magnitude of variation Δ_σ may be examined within lattice QCD by extrapolating $\sigma(t)$ from the physical region $t < 0$. A first attempt has been reported at this conference [29].

3.2. π-N σ term – recent lattice results

In Table 1 we list recent studies of nucleon matrix elements together with parameters of runs.

Results obtained for the connected contribution in the scalar matrix element $\langle N|\bar{u}u + \bar{d}d|N\rangle_{\rm conn.}$ are plotted in Fig. 2, where we used the tadpole-improved renormalization factor in the $\overline{\rm MS}$ scheme at the scale $\mu = 1/a$ given by [32]

$$Z_S \;=\; \left(1 - \frac{3K}{4K_c}\right)\left[1 - 0.0098\alpha_{\overline{\rm MS}}(\frac{1}{a})\right]. \tag{10}$$

The "experimental" value at $(m_\pi/m_\rho)^2 = 0$ equals $\langle N|\bar{u}u + \bar{d}d|N\rangle = \sigma/\hat{m}$ calculated with $\sigma = 45$ MeV and $\hat{m} = 5.5$ MeV. Clearly the connected contribution is too small to account for the experimental value of the π-N σ term.

Previous results for the connected contribution [20,21] are consistent with those in Fig. 2. Estimates from the nucleon mass in quenched QCD using the relation (4) also give consistent values.

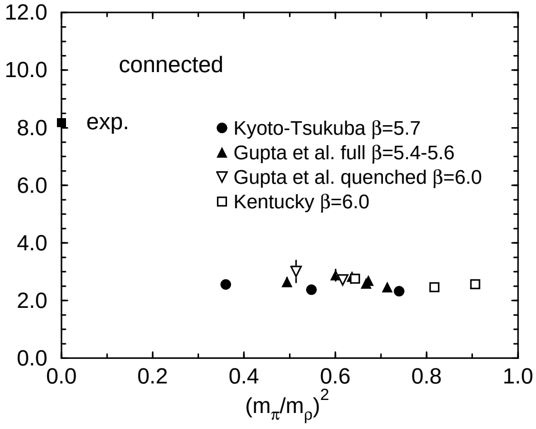

Figure 2. Connected contribution $\langle N|\bar{u}u+\bar{d}d|N\rangle_{\rm conn.}$ for the scalar matrix element as a function of $(m_\pi/m_\rho)^2$. For reference see Table 1.

A direct calculation of the disconnected amplitude (Fig. 1(b)) has been made in quenched QCD using both the wall source method without gauge fixing [11,12] and the Z_2 source method [14,15]. In Fig. 3 results for the R ratio (1) obtained with the wall method [11,12] at $\beta = 5.7$ and $K = 0.164$ ($m_\pi/m_\rho = 0.74$) are plotted. We observe reasonable signals with a linear increase in t for the disconnected amplitude(Fig. 3(a)), albeit errors are significantly larger compared with those for the connected amplitude(Fig. 3(b)).

The disconnected amplitude obtained with the Z_2 source [14,15] at $\beta = 6.0$ and $K = 0.154$ ($m_\pi/m_\rho = 0.80$) is shown in Fig. 4. A reasonable linear increase is also seen for this case.

An important outcome of these calculations is that the disconnected contribution to the scalar matrix element is large, as is clear from a similar magnitude of slope in Fig. 3 (a) and (b). Furthermore the total magnitude of the matrix element obtained by adding the disconnected contribution to the connected one is comparable to the phenomenological estimate. This is shown in Fig. 5 where solid symbols represent total values and open ones the connected contribution duplicated from Fig. 2. A linear extrapolation of quenched results to the chiral limit yields values of the matrix element tabulated in Table 2 (a).

The filled triangles in Fig. 5 represent data obtained in two-flavor full QCD using the nucleon mass derivative dm_N/dm_q [18], showing an

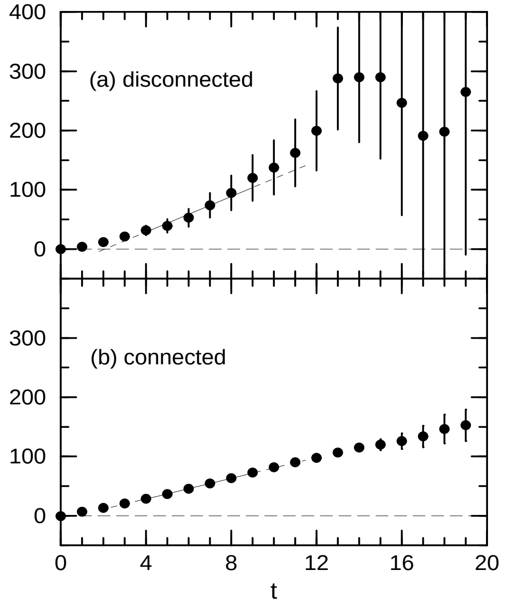

Figure 3. Ratio $R(t)$ for the (a) disconnected and (b) connected amplitudes of the scalar matrix element $\langle N|\bar{u}u+\bar{d}d|N\rangle$ evaluated by the wall source method without gauge fixing [11,12] for K=0.164 at β=5.7 on a $16^3 \times 20$ lattice. Solid lines are linear fits over $4 \le t \le 9$.

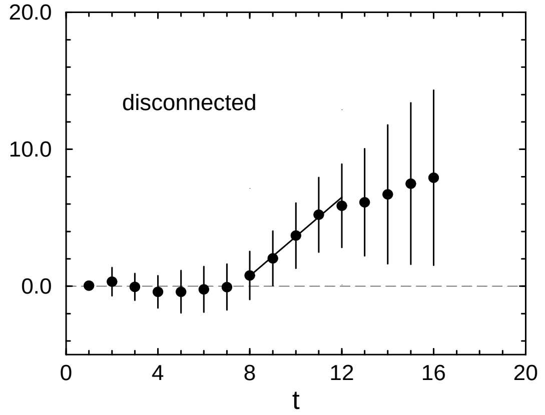

Figure 4. Ratio $R(t)$ for the disconnected amplitude of the scalar matrix element $\langle N|\bar{u}u|N\rangle$ evaluated by the Z_2 source method [14,15] for K=0.154 at β=6.0 on a $16^3 \times 24$ lattice. Solid line is a linear fit over $8 \le t \le 12$.

agreement with quenched estimates (filled circles and diamonds) in the region of heavy quark with $m_\pi/m_\rho > 0.7 - 0.8$.

We find these results to be quite encouraging. On a closer inspection, however, we notice several problems, to which we now turn.

3.3. Problems with scalar matrix elements

3.3.1. physical value of the π-N σ term and quark mass

To convert results for the scalar matrix elements into those for the σ term, we need the value of the quark mass $\hat{m}$ in physical units [33]. In quenched QCD current lattice estimates are $\hat{m} = 5 - 6$MeV for the Wilson quark action, in an agreement with the phenomenological estimation of $\hat{m}$ =5.5MeV. Combined with the total values of the scalar matrix element in Table 2 (a), quenched lattice results for the σ term are consistent with the phenomenological value $\sigma \approx 45$ MeV.

On the other hand, full QCD simulations with the Wilson quark action yield $\hat{m} \approx 2 - 3$MeV (see *e.g.,* Ref. [18]), which are a factor $2 - 3$ smaller than in the quenched case. Since values of matrix elements are similar between the two cases, this means that the σ term is also small $\sigma \approx 20$MeV in full QCD.

Let us add that the σ term estimated from the nucleon mass through (4) in full QCD with the Kogut-Susskind quark action is similarly small $\sigma \approx 20$MeV. For this action the quark mass obtained for quenched and full QCD is consistent, being in the range $\hat{m} \approx 2 - 3$MeV for both cases.

Origin of the small value of quark mass and that of the σ term in full QCD is not clear at present. The discrepancy of quark mass between quenched and full QCD with the Wilson quark action is also not understood.

3.3.2. strange quark content within nucleon

The nucleon matrix element of the strange quark density $\langle N|\bar{s}s|N\rangle$ receives contribution only from the disconnected amplitude. In Table 2 (b) we summarize recent results [12,14]. These values are obtained by extrapolating the valence quark mass to the chiral limit while keeping the strange quark mass fixed at the physical value.

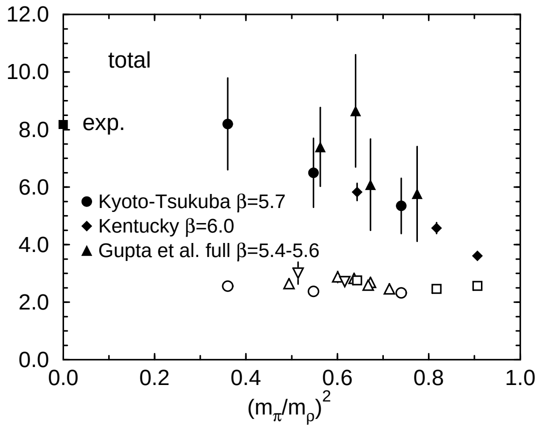

Figure 5. Total amplitude of the scalar matrix element $\langle N|\bar{u}u + \bar{d}d|N\rangle$ as a function of $(m_\pi/m_\rho)^2$. For reference see Table 1. Triangles are full QCD results obtained with the relation (4).

Table 2
Results for nucleon scalar matrix elements

	Ref. [12]	Ref. [14]
(a) $\langle N\|\bar{u}u + dd\|N\rangle$		
connected	2.52(6)	2.85(6)
disconnected	6.2(1.9)	3.79(13)
total	8.9(1.9)	6.6(2)
(b) strangeness content		
$\langle N\|\bar{s}s\|N\rangle$	2.89(61)	1.98(9)
$m_s\langle N\|\bar{s}s\|N\rangle/m_N$	0.40(8)	0.27(1)
$y = \frac{2\langle N\|\bar{s}s\|N\rangle}{\langle N\|\bar{u}u+\bar{d}d\|N\rangle}$	0.65(20)	0.60(4)

Although the strange quark density within nucleon is not directly measurable by experiments, both the ratio $m_s\langle N|\bar{s}s|N\rangle/m_N$, which naively measures the strange quark contribution to the nucleon mass, and the y parameter appear quite large.

Concerning this point Lagaë and Liu suggested [34] that the quark mass correction factor $1+m_q a$ [35], derived for valence quarks nearly on the mass shell, may not adequately account for $O(m_q a)$ effects for sea quarks in disconnected diagrams, which are mostly off the mass-shell states. To examine this possibility they calculated the ratio $\kappa_S(m_q a)$ of the triangle diagram for the operator $\bar{q}q$ with two external gluons at zero momenta on the lattice and in the continuum in one-loop perturbation theory.

In Fig. 6 we compare the $m_s a$ dependence

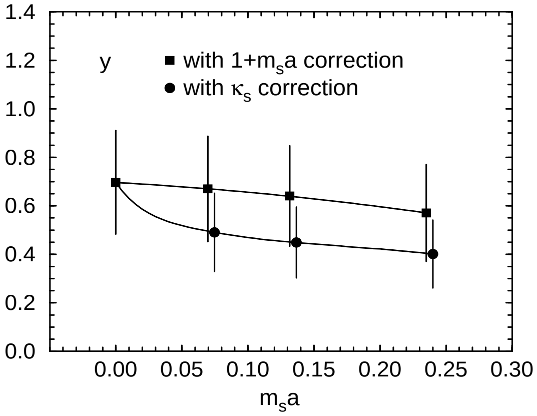

Figure 6. y parameter as functions of $m_s a$ with $1+m_s a$ or $\kappa_S(m_s a)$ factor for strange quark density.

of the y parameter for the data of the Kyoto-Tsukuba group corrected by the $1+m_s a$ factor and by the Lagaë-Liu κ_S factor. With the κ_S factor the y parameter is reduced by about 30% in the region of strange quark mass $m_s a \approx 0.1$, and y values of the Kyoto-Tsukuba and Kentucky groups become $y = 0.46(14)$ and $0.42(3)$. This suggests a possible presence of large $O(m_q a)$ effects for the nucleon matrix element of strange quark density.

3.3.3. baryon mass splitting and reduced matrix elements F_S and D_S

For quenched QCD lattice estimates for the σ term reasonably agree with the phenomenological value. Within the first-order flavor $SU(3)$ breaking formula (7–9), a large value of y is not consistent with this result unless the mass splitting of the baryon octet, or equivalently the matrix element $\langle N|\overline{u}u+\overline{d}d-2\overline{s}s|N\rangle \approx \langle N|\overline{u}u+\overline{d}d|N\rangle_{\rm conn.}$, is small.

To examine this point we recall the definition of reduced matrix elements F_S and D_S given by

$$\begin{aligned}\langle B|\bar{q}\lambda_8 q|B\rangle &= F_S {\rm Tr}(B^\dagger[\lambda_8, B]) \\ &+ D_S {\rm Tr}(B^\dagger\{\lambda_8, B\}). \qquad (11)\end{aligned}$$

To first order in flavor $SU(3)$ breaking, we have the relations $F_S = (M_\Xi - M_N)/2(m_s - \hat{m})$ and $D_S = (M_\Xi + M_N - 2M_\Sigma)/2(m_s - \hat{m})$, from which we find experimentally that

$$F_S^{\rm exp.} = 1.52, \qquad D_S^{\rm exp.} = -0.518. \qquad (12)$$

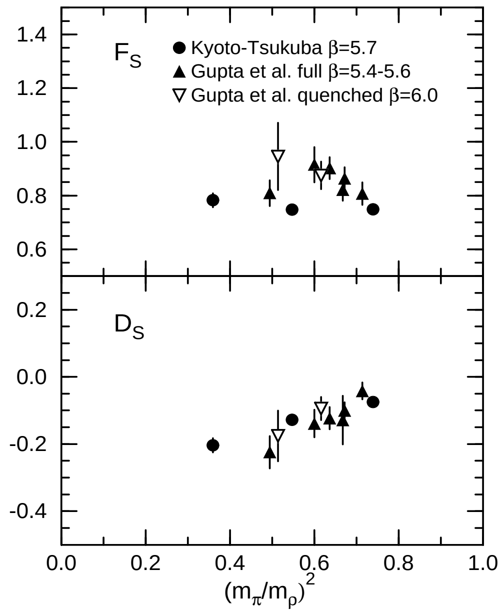

Figure 7. Reduced scalar matrix elements F_S and D_S. For reference see Table 1.

These values are to be compared with lattice estimates obtained from the relations,

$$\begin{aligned}F_S &= \frac{1}{2}\langle N|\bar{u}u|N\rangle_{\rm conn.} \\ D_S &= \frac{1}{2}\langle N|\bar{u}u - 2\bar{d}d|N\rangle_{\rm conn.} \qquad (13)\end{aligned}$$

where only connected contributions are kept since disconnected contributions are to be ignored to leading order of flavor symmetry breaking.

Lattice results from the studies in Table 1 are plotted in Fig. 7. Previous estimates [20,21] are similar with results in this figure. While there may be some trend of increase toward the chiral limit, both matrix elements are small compared to experiments. It should be added that the ratio F_S/D_S is consistent, however.

One can estimate the baryon mass splitting from results for the reduced matrix elements. At $\beta = 5.7$, for example, one finds $M_\Xi - M_N = 177(8)$MeV and $M_\Sigma - M_N = 114(5)$MeV [12] as compared to the experimental values 379MeV and 254MeV. On the other hand, a recent spectrum calculation at $\beta = 6.0$ on a $32^3 \times 64$ lattice reported $M_\Xi - M_N = 300(27)$MeV and $M_\Sigma - M_N = 185(17)$MeV [36], which show a much

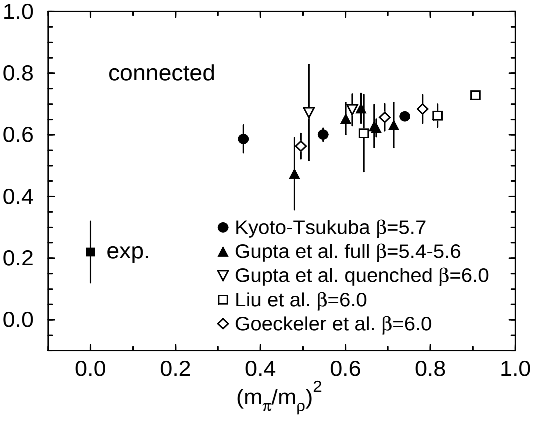

Figure 8. Connected contribution $\Delta\Sigma_{\rm conn.} = (\Delta u + \Delta d)_{\rm conn.}$ of the axial vector matrix element as a function of $(m_\pi/m_\rho)^2$. For reference see Table 1.

better agreement with experiments.

Systematic analyses calculating both the scalar matrix elements and the baryon mass splitting within the same simulation have not been carried out so far. These are needed to elucidate the origin of the problem in these quantities, especally to see whether it can be ascribed to a large violation of scaling.

4. NUCLEON AXIAL VECTOR MATRIX ELEMENTS

4.1. Quark content of proton spin

The forward matrix element of the axial vector current $\bar{q}\gamma_\mu\gamma_5 q$ measures the contribution Δq of a given quark flavor q to the spin of the proton,

$$\langle P_s|\bar{q}\gamma_3\gamma_5 q|P_s\rangle = s\cdot\Delta q, \qquad (14)$$

where $|P_s\rangle$ is the proton state at rest with the spin projection in the z direction equal to $s/2$. Recent experiments on polarized deep inelastic lepton-nucleon scattering from SMC [37] and E143 [38] have confirmed the earlier finding of EMC [39] that the fraction of proton spin carried by quarks has a small value $\Delta\Sigma = \Delta u + \Delta d + \Delta s \approx 0.2 - 0.3$ and that the strange quark contribution is non-vanishing and negative $\Delta s \approx -0.1$. These values are quite different from naive expectations from quark models. We tabulate the experimental values and those from quark models in Table 3 (a) and (b).

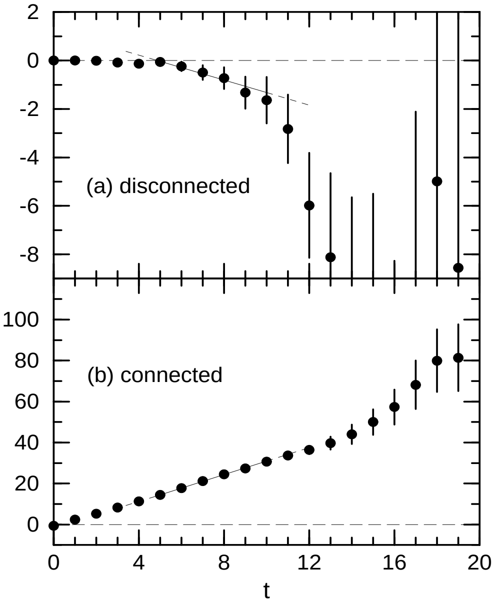

Figure 9. Ratio $R(t)$ for the (a) disconnected and (b) connected amplitudes of the axial vector matrix element Δu evaluated by the wall source method without gauge fixing [11,13] for K=0.164 at β=5.7 on a $16^3 \times 20$ lattice. Solid lines are linear fits over $5 \le t \le 10$.

Recent lattice results for the connected contribution $\Delta\Sigma_{\rm conn.} = (\Delta u + \Delta d)_{\rm conn.}$ are compiled in Fig. 8 where we used the tadpole-improved renormalization factor given by [32]

$$Z_A \;=\; \left(1 - \frac{3K}{4K_c}\right)\left[1 - 0.31\alpha_{\overline{\rm MS}}(\frac{1}{a})\right]. \qquad (15)$$

Lattice parameters for individual runs are summarized in Table 1. For comparison we also plot the experimental value of SMC at $(m_\pi/m_\rho)^2 = 0$. The connected contribution alone is too large to explain the small value of $\Delta\Sigma$.

In Fig. 9 we show results for the R ratio (1) for the up quark contribution from Ref. [11,13] where the disconnected contribution (Fig. 9(a)) is obtained with the method of wall source without gauge fixing. Compared to the case of the scalar matrix element, the data for the disconnected contribution are much noisier. The negative value of the matrix element, not predictable in quark models, is clearly observed, however. A similar trend is also seen in the result obtained with the Z_2 source shown in Fig. 10 [14,15].

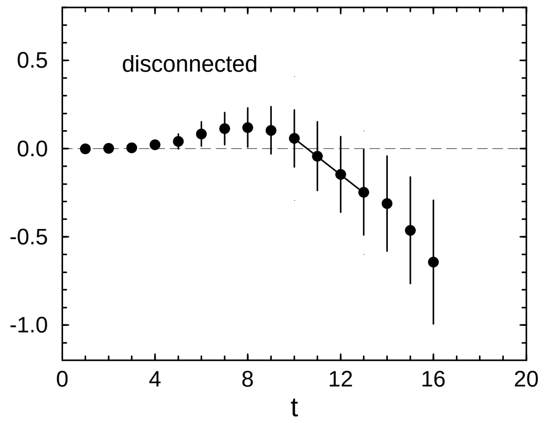

Figure 10. Ratio $R(t)$ for the disconnected amplitude of the axial vector matrix element Δu evaluated by the Z_2 source method [14,15] for K=0.154 at β=6.0 on a $16^3\times 24$ lattice. Solid line is a linear fit over $10 \le t \le 13$.

Table 3
Axial vector matrix elements from (a) experiments, (b)quark models and (c) lattice calculations.

	Δu	Δd	Δs	$\Delta\Sigma$
(a) Experiment				
SMC [37]	0.80(6)	-0.46(6)	-0.12(4)	0.22(10)
E143 [38]	0.82(6)	-0.44(6)	-0.10(4)	0.27(10)
(b) Quark model				
non-rel.	4/3	-1/3	0	1
rel.	1.01	-0.25	0	0.76
(c)Lattice results at $m_q = 0$				
Ref. [13]	0.638(54)	-0.347(46)	-0.109(30)	0.18(10)
Ref. [15]	0.79(11)	-0.42(11)	-0.12(1)	0.25(12)

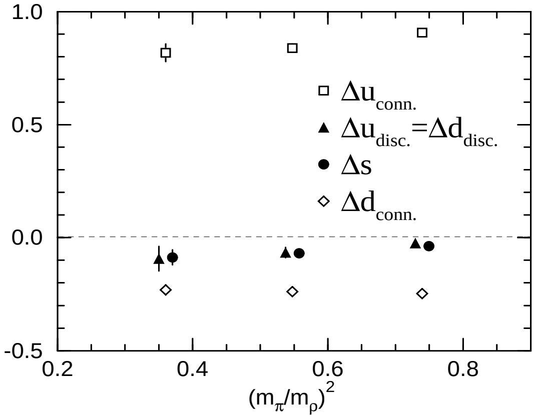

Figure 11. Axial-vector matrix elements for u, d and s quarks as functions of $(m_\pi/m_\rho)^2$ [13]. Strange quark mass is fixed to the physical value.

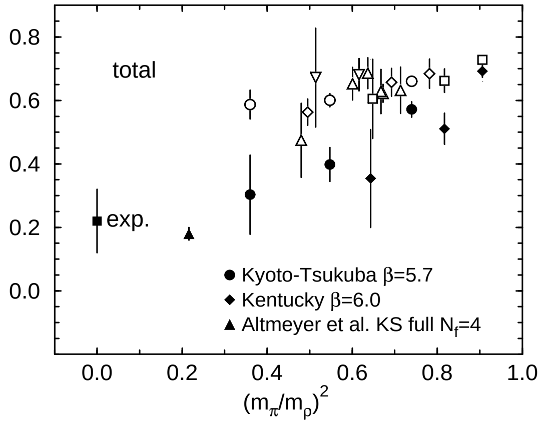

Figure 12. Total value of $\Delta\Sigma$ as a function of $(m_\pi/m_\rho)^2$. For reference see Table 1. Triangle is a result using the anomaly equation (5).

Values of the connected and disconnected contributions obtained in ref. [13] are plotted in Fig. 11 for u, d and s quarks separately as functions of $(m_\pi/m_\rho)^2$. The magnitude of disconnected contributions is small for each quark. However, the total amplitude $\Delta\Sigma$ receives a negative disconnected contribution from u, d and s quarks. As a result the value of $\Delta\Sigma$ is significantly reduced from that obtained from connected contributions alone. This is shown in Fig. 12 where filled symbols are the total amplitude and open ones connected contributions taken from Fig. 8. We observe that the total amplitude points toward the experimental value for light quarks.

A more detailed comparison is made in Table 3 where the total contribution extrapolated to $m_q = 0$ is listed for each quark. Lattice results are in reasonable agreement with those from experiments.

4.2. Isovector axial coupling g_A

The $SU(3)$ reduced matrix elements for the axial vector current are given by

$$F_A = \frac{1}{2}(\Delta u)_{\rm conn.} \tag{16}$$

$$D_A = \frac{1}{2}(\Delta u - 2\Delta d)_{\rm conn.}\,. \tag{17}$$

Experimental values of these matrix elements are deduced using neutron β decay, which gives a very precise value of the isovector axial coupling g_A,

$$g_A^{\mathrm{exp.}} = F_A + D_A = 1.2573(28) \tag{18}$$

and hyperon β decay, which yields

$$F_A - D_A = -0.327(20). \tag{19}$$

From the two estimates one finds for the ratio,

$$F_A/D_A = 0.58(5) \tag{20}$$

In Fig. 13 we plot recent lattice results for g_A and the ratio F_A/D_A. We see that lattice data for g_A are consistently smaller than the experimental value by about 20-30 % toward light quarks, while the ratio F_A/D_A is consistent.

We remark that a previous result [21] for a $\sqrt{3}$-blocked quark action shows a simiar trend if a tadpole-improved renormalization factor appropriate for the action is employed.

The disagreement of g_A represents another problem with flavor non-singlet nucleon matrix elements. It does not seem to arise from the effect of quenching since full QCD estimates plotted by upward triangles [18] do not deviate from quenched results. Effects of scaling violations also seem small since results from two values of β at 5.7 [13] and at 6.0 [18,30,31] are in agreement. One may suspect a possible ambiguity in the choice of the renormalization constant Z_A, especially because the ratio F_A/D_A agrees with experiments. However, the same renormalization factor enters in a calculation of the pion decay constant f_π, for which quenched lattice results at $\beta = 5.7 - 6.0$ agree with the experimental value within about 10%. Furthermore a non-perturbatively determined value of Z_A obtained at $\beta = 6.0$ and $K = 0.1515$ and 0.153 is quite consistent with the perturbative result (15) [40].

5. HADRON SCATTERING LENGTH

The theoretical basis for a lattice calculation of hadron scattering lengths is the formula proven by Lüscher [41]; it relates the s-wave scattering length a_0 to the energy level E of the lightest two-hadron state with vanishing spatial momentum in a cubic box of length L according to

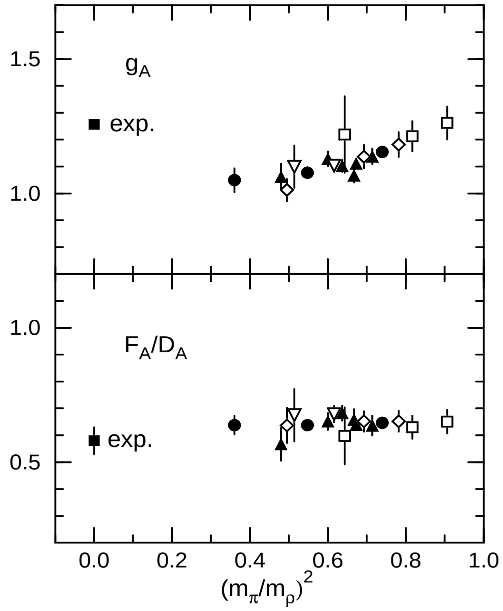

Figure 13. Isovector axial coupling g_A and F_A/D_A as functions of $(m_\pi/m_\rho)^2$. For the meaning of symbols see Fig. 8.

$$E - 2m = -\frac{4\pi a_0}{mL^3}\left(1 + c_1\frac{a_0}{L} + c_2\frac{a_0^2}{L^2}\right) + O\left(\frac{1}{L^6}\right) \tag{21}$$

with $c_1 = -2.837297$ and $c_2 = 6.375183$. The technical difficulty of calculating general four-point functions (including disconnected ones) needed for an extraction of the energy level E was overcome by the wall source method without gauge fixing, and π-π, π-N, K-N and N-N scattering lengths have been calculated in quenched QCD [3,8,9]. While no new simulations have been carried out since *LATTICE 93*, two theoretical studies aiming at a deeper understanding of the lattice calculation of hadron scattering lengths have been made (see also Refs. [42,43] for related investigations).

5.1. π-π scattering length

Chiral perturbation theory suggests that quantities calculated in quenched QCD often develop spurious infrared divergences in the chiral limit, which are not present in full QCD [44]. Bernard and Golterman [22] investigated the effect of quenching in the energy level E of the two-pion

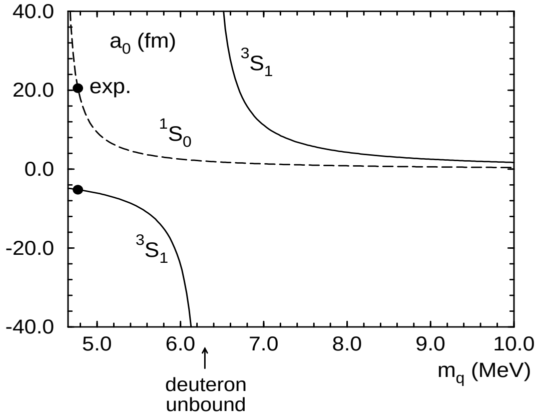

Figure 14. N-N scattering length a_0 calculated by a one-boson exchange model for ${}^1S_0$ and ${}^3S_1$ channels as functions of quark mass m_q. The physical point corresponds to $m_q = 4.8$ MeV.

state using quenched chiral perturbation theory technique, extending a previous work on the subject [45]. They found that enhanced finite-volume corrections of order $L^0 = 1$ and L^{-1} occur in E at one loop due to the double pole in the η' propagator. This implies that it is not consistent to use Lüscher's formula in quenched QCD.

On the other hand, a quenched lattice calculation of π-π scattering lengths with the Kogut-Susskind quark action [3] yielded results consistent with the prediction of current algebra and PCAC, which is known to hold for the Kogut-Susskind case [46]. They suggest that this agreement is due to an accidental choice of lattice parameters such that the enhanced finite-volume corrections are not large for the values of $m_\pi L$ of the simulation.

5.2. N-N scattering length

The nucleon-nucleon scattering length is a fundamental parameter characterizing the low-energy properties of the nuclear force. Experimentally they are well determined and are known to have large values,

$$\begin{aligned} a_0({}^1S_0) &= +20.1(4) \text{ fm}, \\ a_0({}^3S_1) &= -5.432(5) \text{ fm}. \end{aligned} \tag{22}$$

Since there are no constraints from chiral symmetry for N-N scattering, explaining these values from first principles of lattice QCD is an interesting dynamical problem. However, a number of obstacles exist toward realistic calculations. A very large lattice is needed to apply Lüscher's formula in order to suppress $O(L^{-6})$ corrections neglected in (21). Extraction of the scattering length in the ${}^3S_1$ channel requires a calculation of the lowest scattering state orthogonal to the ground state, which is the deuteron bound state.

A possible strategy in this situation would be to examine the quark mass dependence of the scattering lengths starting from a heavy quark where simulations are much easier. For this approach we need to understand the behavior of scattering lengths for heavy quarks.

For heavy quarks the N-N interaction becomes shorter ranged since pions exchanged between nucleons are heavier. This will force the nucleons out of the attractive well of the potential, which suggests that the deuteron becomes unbound as the quark mass increases.

A closer examination of this possibility was made in Ref. [9], taking a phenomenological model of one-boson exchange potentials [47] and varying hadron masses in the model as a function of quark mass according to lattice data. The results for the N-N scattering lengths are plotted in Fig. 14. The divergence of the scattering length for the ${}^3S_1$ channel taking place at $m_q = 6.3$ MeV signals unbinding of the deuteron. For $m_q > 6.3$ MeV, both $a_0({}^1S_0)$ and $a_0({}^3S_1)$ are positive and rapidly decrease to have values of order 1 fm. Also the value of $a_0({}^3S_1)$ is larger than that for $a_0({}^1S_0)$ for heavy quark indicating a stronger attraction in the ${}^3S_1$ channel.

These are precisely the features found in a lattice calculation of N-N scattering lengths [8,9]. The results are shown in Fig. 15 together with those for π-π and π-N cases for comparison.

6. CONCLUSION

In the last two years, a substantial progress has been made in the lattice QCD study of the flavor singlet nucleon matrix elements. Applications of efficient calculational techniques for handling disconnected quark loop amplitudes revealed significant sea quark contributions in the flavor singlet scalar and axial vector matrix el-

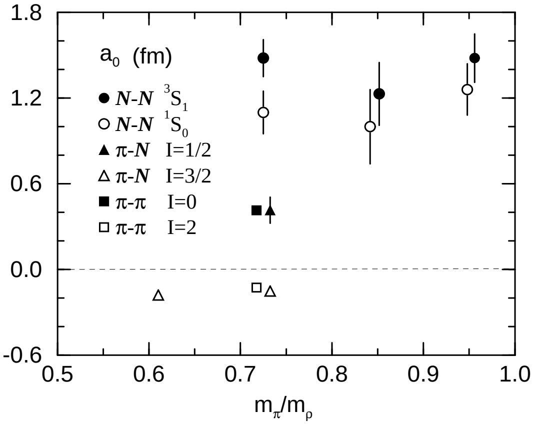

Figure 15. N-N scattering length in physical units at β=5.7 on a 20^4 lattice. Also shown are the π-π and π-N scattering lengths at the same β on an $12^3 \times 20$ lattice.

ements. Adding sea and valence quark contributions the total magnitude of these matrix elements are comparable to experimental estimates. Although the nature of systematic errors such as scaling violations and quenching effects need to be understood more precisely, the encouraging results found so far point toward an eventual resolution of the problems related to the flavor singlet matrix elements within lattice QCD.

In the course of the studies it has become apparent that current lattice results for flavor non-singlet scalar and axial vector matrix elements differ from experiments beyond statistical errors. A systematic scaling study appears needed to pinpoint the origin of the problem.

We have also discussed some recent work in the study of hadron scattering lengths. The model result that the deuteron becomes unbound for a quark mass only slightly larger than the physical value suggests that much interesting physics can be done on the subject of N-N scattering. At the same time the possibility of a severe quenching error pointed out for the π-π case signifies the need of caution in the use of quenched QCD.

Study of flavor singlet physics is a young subject in lattice QCD. Results obtained so far should serve as a stepping stone for further development in this area in the years to come.

Acknowledgements

I would like to thank C. Bernard, S. Dong, M. Fukugita, Y. Kuramashi, K. Liu, G. Schierholz and A. Ukawa for correspondence and discussions. Valuable suggestions of A. Ukawa on the manuscript are gratefully acknowledged. This work is supported in part by the Grant-in-Aid of the Ministry of Education (No. 05640363).

REFERENCES

1. M. Fukugita, T. Kaneko and A. Ukawa, Phys. Lett. B145 (1984) 93.
2. S. Itoh, Y. Iwasaki and T. Yoshié, Phys. Rev. D36 (1987) 527.
3. Y. Kuramashi, M. Fukugita, H. Mino, M. Okawa and A. Ukawa, Phys. Rev. Lett. 71 (1993) 2387.
4. R. D. Kenway, in *Proc. XXII Int. Conf. on High Energy Physics*, eds. A. Meyer and E. Wieczorek (Leipzig, 1984) vol. 1, p. 51; A. Billoire, E. Marinari and G. Parisi, Phys. Lett. B162 (1985) 160.
5. R. T. Scalettar *et al.*, Phys. Rev. B34 (1986) 7911; S. Duane and J. B. Kogut, Nucl. Phys. B275 (1986) 398; G. G. Batrouni *et al.*, Phys. Rev. D32 (1985) 2736; S. Gottlieb *et al.*, ibid. 35 (1987) 3972.
6. S. J. Dong and K. F. Liu, *Lattice 91*, Nucl. Phys. B (Proc. Suppl.) 26 (1992) 353; *Lattice 92*, Nucl. Phys. B (Proc. Suppl.) 30 (1993) 487; Phys. Lett. B328 (1994) 130.
7. Y. Kuramashi, M. Fukugita, H. Mino, M. Okawa and A. Ukawa, Phys. Rev. Lett. 72 (1994) 3448; M. Fukugita, Y. Kuramashi, M. Okawa and A. Ukawa, Phys. Rev. D51 (1995) 3952.
8. M. Fukugita, Y. Kuramashi, H. Mino, M. Okawa and A. Ukawa, Phys. Rev. Lett. 73 (1994) 2176.
9. M. Fukugita, Y. Kuramashi, M. Okawa, H. Mino and A. Ukawa, Phys. Rev. D52 (1995) 3003.
10. Y. Kuramashi, M. Fukugita, H. Mino, M. Okawa and A. Ukawa, *Lattice 93*, Nucl. Phys. B (Proc. Suppl.) 34 (1994) 117.
11. M. Fukugita, Y. Kuramashi, M. Okawa and A. Ukawa, *Lattice 94*, Nucl. Phys. B (Proc. Suppl.) 42 (1995) 334.
12. M. Fukugita, Y. Kuramashi, M. Okawa and

A. Ukawa, Phys. Rev. D51 (1995) 5319.

13. M. Fukugita, Y. Kuramashi, M. Okawa and A. Ukawa, Phys. Rev. Lett. 75 (1995) 2092.
14. S. J. Dong and K. F. Liu, *Lattice 94*, Nucl. Phys. B (Proc. Suppl.) 42 (1995) 322.
15. S. J. Dong, J. -F. Lagaë and K. F. Liu, Phys. Rev. Lett. 75 (1995) 2096.
16. R. Altmeyer, M. Göckeler, R. Horsley, E. Laermann and G. Schierholz, *Lattice 93*, Nucl. Phys. B (Proc. Suppl.) 34 (1994) 376.
17. R. Altmeyer, M. Göckeler, R. Horsley, E. Laermann and G. Schierholz, Phys. Rev. D49 (1994) R3087.
18. R. Gupta, C. F. Baillie, R. G. Brickner, G. W. Kilcup, A. Patel and S. R. Sharpe, Phys. Rev. D44 (1991) 3272.
19. R. Gupta and J. E. Mandula, Phys. Rev. D50 (1994) 6931 and previous references cited therein.
20. L. Maiani, G. Martinelli, M. L. Paciello and B. Taglienti, Nucl. Phys. B293 (1987) 420.
21. S. Güsken, K. Schilling, R. Sommer, K.-H. Mütter and A. Patel, Phys. Lett. B212 (1988) 216; ibid. B227 (1989) 266; Nucl. Phys. B327 (1989) 763.
22. C. W. Bernard and M. F. L. Golterman, Washington preprint Wash. U. HEP/95-61 (1995); in these proceedings.
23. C. Bernard, T. Draper, G. Hockney, and A. Soni, in *Lattice Gauge Theory: A Challenge in Large-Scale Computing*, eds. B. Bunk *et al.* (Plenum, New York, 1986)p. 199; G. W. Kilcup, S. R. Sharpe, R. Gupta, G. Guralnik, A. Patel and T. Warnock, Phys. Lett. B164 (1985) 347.
24. See, for example, G. P. Lepage, in *Proc. of TASI'89 Summer School*, eds. T. DeGrand and D. Toussaint (World Scientific, Singapore, 1990) p. 97.
25. R. Koch, Z. Phys. C15 (1982) 161.
26. J. Gasser, H. Leutwyler and M. E. Sainio, Phys. Lett. B253 (1991) 252.
27. See, *e.g.*, C. A. Dominguez and P. Langacker, Phys. Rev. D24 (1981) 1905.
28. J. Gasser, Ann. Phys. (N. Y.) 136 (1981) 62.
29. S. J. Dong and K. F. Liu, in these proceedings.
30. K. F. Liu, S. J. Dong, T. Draper, J. M. Wu and W. Wilcox, Phys. Rev. D49 (1994) 4755.
31. M. Göckeler, R. Horsley, M. Ilgenfritz, H. Perlt, P. Rakow, G. Schierholz and A. Schiller, *Lattice 94*, Nucl. Phys. B (Proc. Suppl.) 42 (1995) 337; DESY preprint DESY 95-128 (1995).
32. G. P. Lepage and P. B. Mackenzie, Phys. Rev. D48 (1993) 2250.
33. For a review and references, see, A. Ukawa, *Lattice 92*, Nucl. Phys. B (Proc. Suppl.) 30 (1993) 3; R. Gupta, *Lattice 94*, Nucl. Phys. B (Proc. Suppl.) 42 (1995) 85.
34. J. -F. Lagaë and K. F. Liu, *Lattice 94*, Nucl. Phys. B (Proc. Suppl.) 42 (1995) 355; Kentucky preprint UK/94-04 (1994).
35. G. P. Lepage, *Lattice 91*, Nucl. Phys. B (Proc. Suppl.) 26 (1992) 45.
36. T. Bhattacharya and R. Gupta, *Lattice 94*, Nucl. Phys. B (Proc. Suppl.) 42 (1995) 935.
37. D. Adams *et al.* (SMC), Phys. Lett. B329 (1994) 399.
38. K. Abe *et al.* (E143), Phys. Rev. Lett. 74 (1995) 346.
39. J. Ashman *et al.* (EMC), Phys. Lett. B206 (1988) 364.
40. M. Göckeler, R. Horsley, M. Ilgenfritz, H. Perlt, P. Rakow, G. Schierholz and A. Schiller, in these proceedings.
41. M. Lüscher, Commun. Math. Phys. 105 (1986) 153; Nucl. Phys. B354 (1991) 531; Nucl. Phys. B364 (1991) 237.
42. H. R. Fiebig, O. Linsuain, H. Markum and K. Rabitsch, in these proceedings and references cited therein.
43. K. Rummukainen and S. Gottlieb, Nucl. Phys. B450 (1995) 397; in these proceedings.
44. C. W. Bernard and M. F. L. Golterman, Phys. Rev. D46 (1992) 853; S. R. Sharpe, ibid. 46 (1992) 3146.
45. C. W. Bernard, M. F. L. Golterman, J. Labrenz, S. R. Sharpe and A. Ukawa, *Lattice 93* Nucl. Phys. B (Proc. Suppl.) 34 (1994) 334.
46. S. R. Sharpe, R. Gupta and G. W. Kilcup, Nucl. Phys. B383 (1992) 309.
47. K. Holinde, K. Erkelenz and R. Alzetta, Nucl. Phys. A194 (1972) 161; A198 (1972) 598.